ACS APPLIED MATERIALS & INTERFACES

Research Article

www.acsami.org

Succinonitrile as a Corrosion Inhibitor of Copper Current Collectors for Overdischarge Protection of Lithium Ion Batteries

Young-Soo Kim,[†] Seon-Ha Lee,[‡] Mi-Young Son,[∥] Young Mee Jung,[§] Hyun-Kon Song,*[,†] and Hochun Lee*[,‡]

[†]Department of Energy Engineering and Department of Chemical Engineering, Ulsan National Institute of Science and Technology (UNIST), Ulsan 689-798, South Korea

[‡]Department of Energy Systems Engineering, Daegu Gyeongbuk Institute of Science and Technology (DGIST), Daegu 711-873, South Korea

[§]Department of Chemistry, Kangwon National University, Chunchon 200-701, South Korea

[∥]Batteries R&D, LG Chem Ltd., Daejeon 305-380, South Korea

Supporting Information

ABSTRACT: Succinonitrile (SN) is investigated as an electrolyte additive for copper corrosion inhibition to provide overdischarge (OD) protection to lithium ion batteries (LIBs). The anodic Cu corrosion, occurring above 3.5 V (vs Li/Li^+) in conventional LIB electrolytes, is suppressed until a voltage of 4.5 V is reached in the presence of SN. The corrosion inhibition by SN is ascribed to the formation of an SN-induced passive layer, which spontaneously develops on the copper surface during the first anodic scan. The passive layer is composed mainly of $Cu(SN)_2PF_6$ units, which is evidenced by Raman spectroscopy and electrochemical quartz crystal microbalance measurements. The effects of the SN additive on OD protection are confirmed by using 750 mAh pouch-type full cells of $LiCoO_2$ and graphite with lithium metal as a reference electrode. Addition of SN completely prevents corrosion of the copper current collector in the full cell configuration, thereby tuning the LIB chemistry to be inherently immune to the OD abuses.

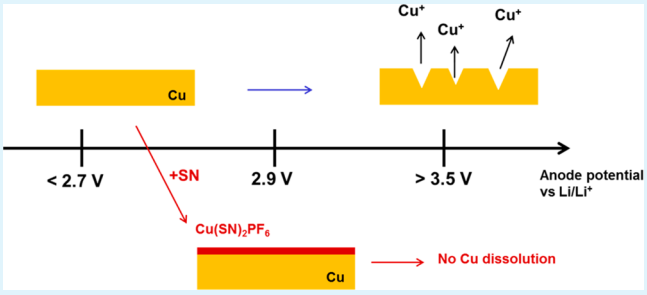

KEYWORDS: *overdischarge, corrosion inhibitor, succinonitrile, copper current collector, lithium ion batteries*

INTRODUCTION

The demand for lithium ion batteries (LIBs) has rapidly increased in various fields, from portable IT devices to emerging applications such as electric vehicles and renewable energy storage.[1] The long-term stability of LIBs, however, still remains an issue and becomes more serious in the new applications where a cycle life of more than 10 years is required. With appreciable success, a great deal of effort has been devoted to improving the reliability of LIBs under various abusive conditions, including overcharge, high-temperature cycling and storage, and mechanical stress. Cyclohexyl benzene[2] and biphenyl[3] were used for overcharge protection. The thermal stability was significantly enhanced with the help of propane sultone[4] and succinonitrile.[5] Nonflammability was achieved by using vinyl-tris(methoxydiethoxy)silane[6] as a flame retardant. In contrast, much less attention has been paid to overdischarge (OD) issues, which are particularly critical in middle-scale to large-scale devices where failure in a single cell leads to the shut down of all cells within a connection in series.[7−13]

State-of-the-art LIBs are inherently vulnerable to OD abuse because they are designed to have anode-limiting configurations to prevent the possible deposition of Li at the anode.[7] In the configuration, anode potential is bound to increase to meet cathode potential during an OD event (Figure 1). The abnormal rise of the anode potential can damage the solid electrolyte interphase (SEI) layer existing on anodes, leading to additional electrolyte decomposition and thus capacity fading.[14−16] More importantly, as the anode potential nears ~3.5 V (vs Li/Li^+), anodic corrosion of the copper current collector is triggered, inducing damage such as electric shunt formation, contact resistance rise, and total block-off of cells.[7−13]

One way of protecting cells from OD is to tune LIBs into a cathode-limiting configuration by altering the cell balance (the ratio of anode to cathode capacities). We reported an OD protection strategy for tailoring the first-cycle columbic efficiency of the cathode by employing Li_2NiO_2 as a cathode additive that exhibits a distinctively huge irreversible capacity at the first cycle.[13] Utilization of the cathode additive, however,

Received: November 14, 2013
Accepted: January 20, 2014
Published: January 20, 2014

   dx.doi.org/10.1021/am405092y | ACS Appl. Mater. Interfaces 2014, 6, 2039−2043

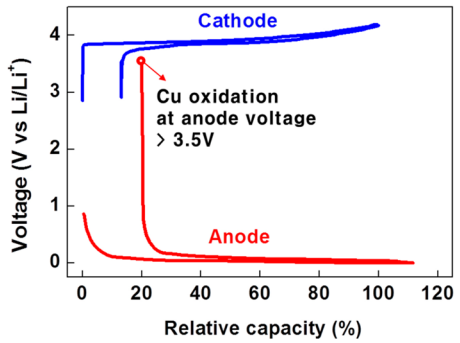

Figure 1. Potential profiles of a conventional LIB of anode-limiting configuration during charge and discharge. The arrow denotes the terminal point at the end of overdischarge to 0 V of cell voltage.

necessitates modification of the process of fabrication of cathode electrodes as well as an overall redesign of cell balance. An alternative simpler strategy is to use electrolyte additives. Introduction of redox shuttles (RS) into the electrolyte suppressed the abnormal anode voltage rise by repetitive redox cycles.[12] However, the RS additives limit cathode voltage as well, so that its application is limited only to the LIBs employing low-voltage cathode materials such as $LiFePO_4$. Besides the RS additives, compounds that inhibit copper corrosion can be used as electrolyte additives for OD protection. To develop copper corrosion inhibitors for organic electrolytes of LIBs, we could learn lessons from extensive studies of the inhibition of copper corrosion in aqueous solutions.[17−21] However, most inhibitors effectively used in aqueous solutions are strongly electron-donating compounds, so that they are too unstable to be served as inhibitors in LIB applications.[17,19]

In our previous study, we reported on an organo−transition metal interaction induced by the electronegativity of succinonitrile (SN).[5] The interaction led to an outstanding thermal stability without any adverse effects on cell performance. The SN-induced stability was attributed to formation of a strong bond between SN and transition metals (Co) on the cathode surface. In this study, we examined the SN as an electrolyte additive for OD protection and expected that SN coordinates with Cu ions to form a passive layer on the surface of copper current collectors.

EXPERIMENTAL SECTION

Chemicals. A mixture of ethylene carbonate (EC) and ethylmethyl carbonate (EMC) [1/2 (v/v)] or EC and diethyl carbonate (DEC) [1/2 (v/v)] with 1 M $LiPF_6$ was used as an electrolyte of LIB cells (LG Chem). SN (Aldrich) and 3-fluoroethylene carbonate (FEC) (Soulbrain) were used as received.

Electroanalysis. A three-electrode configuration was employed for investigating basic corrosion electrochemistry with Li foil and Pt wire as reference and counter electrodes, respectively. A copper disk (area of 0.20 cm^2) or a 9 MHz AT-cut Cu-plated quartz crystal (area of 0.20 cm^2) was used as a working electrode. Prior to the experiments, the Cu disk electrode was abraded with a 1200-grit SiC paper while the Cu-plated quartz crystal was rinsed with acetone and immersed in an electrolyte for 10 min. Electrochemical experiments were conducted with a Biologic VSP instrument. The electrochemical quartz crystal microbalance (EQCM) experiments were performed with a Princeton Applied Research QCM922 instrument connected to the potentiostat. The potential of the copper disk electrode was scanned at a rate of 20 mV s^{-1} via linear sweep voltammetry (LSV), while a rate of 10 mV s^{-1} was used in EQCM experiments. All electrochemical experiments were performed in an Ar atmosphere glovebox (H_2O and O_2 concentrations of <5 ppm and 25 ± 2 °C).

Raman Spectroscopy. Raman spectra were recorded using a Jobin Yvon/HORIBA LabRam ARAMIS Raman spectrometer. The radiation from an air-cooled frequency-doubled Nd:Yag laser (532 nm) was used as an excitation source. Raman scattering was detected in a 180° geometry by a multichannel air-cooled (−70 °C) charge-coupled device (CCD) camera (1024 × 256 pixels). For Raman sample preparation, Cu foil electrodes were polarized in an electrolyte by sweeping from an open circuit voltage to 3.1 V that is higher than the peak voltage. After polarization, the Cu samples were washed with DMC and dried inside a glovebox.

Overdischarge Tests of LIB Cells. The 750 mAh Al pouch full cells were employed with lithium metal as a reference electrode. Cathodes were prepared by coating a mixture of $LiCoO_2$ (KD10, Umicore), 2 wt % Super-P, and 3 wt % polyvinylidene fluoride (PVdF) binder on aluminum foil (15 μm, Sam-A aluminum). Anodes were prepared by coating a mixture of natural graphite (DAG-87, Sodiff), 1.5 wt % styrene-butadiene rubber (SBR), and 1 wt % carboxymethyl cellulose (CMC) binder on copper foil (10 μm, LS cable and system). Lithium metal foil (1 cm^2) tightly pressed on Cu mesh was used as the reference electrode that was placed on one side of the pouch cells. A solution of 1 M $LiPF_6$ in an EC/EMC mixture [1/2 (v/v)] with 2 wt % FEC was used as the base electrolyte.

The assembled pouch cells were initially charged at 0.05 C and aged for 5 days at room temperature to complete the formation process. The cells were galvanostatically charged at 0.2 C while the cell potential was held at 4.2 V and then galvanostatically discharged at 0.2 C. Then, the cells were degassed and resealed inside a vacuum chamber to eliminate gases evolved during the formation process. Before the overdischarge test, the cells were cycled several times over in a potential range between 3 and 4.2 V. Cells was overdischarged galvanostatically at 300 mA to 3 V of the cathode versus anode, 3 mA to 2.7 V, and finally 1 mA to 0 V. Potentials of cathode versus reference, anode versus reference, and cathode versus anode were monitored independently during overdischarge. Discharge capacities at 0.2 C were compared between before and after three consecutive overdischarges.

RESULTS AND DISCUSSION

SN-Induced Passivation of Cu for Corrosion Inhibition. Inhibitive effects of SN on anodic Cu corrosion were assessed by using linear sweep voltammetry (LSV). In the SN-absent electrolyte as a control (Figure 2), a steep increase in the oxidation current responsible for massive Cu oxidation was observed above 3.5 V. However, the anodic behavior of Cu changed significantly in the presence of SN. Even if the oxidation current starts to increase as early as 2.8 V, further Cu oxidation was significantly suppressed after showing a peak current around 2.9 V. The oxidation stability of Cu was

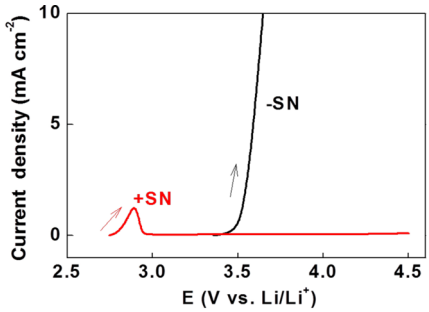

Figure 2. Linear sweep voltammograms (LSVs) of copper electrodes with 1 M $LiPF_6$ in an EC/DEC mixture [1/2 (v/v)] containing no additive (−SN) or 3 wt % SN (+SN). The scan rate was 20 mV s^{-1}.

extended to the potential as high as 4.5 V by the SN addition. It seems informative to consider that the similar voltammetric behaviors are observed with corrosion inhibitors in aqueous solutions. Copper exhibits an anodic peak followed by subsequent inhibition in aqueous solutions of organic acids.[18,21] The anodic peak is attributed to formation of a Cu_2O or Cu oxalate layer that suppresses further Cu oxidation.[19,20] In nonaqueous LIB electrolytes, however, the additive-induced passivation of Cu leading to corrosion prevention has not been studied thoroughly to the best of our knowledge.[11,22−26]

The chemical nature of the SN-induced passivation was examined using Raman spectroscopy, based on the idea that a passive surface layer is formed by the interaction of SN with Cu occurring around the anodic peak potential (Figure 2). A copper electrode was subjected to anodic polarization at a potential higher than the peak position (2.9 V) in the SN-present electrolyte. Two possible modes of interaction between SN and the Cu surface are expected. First, SN is chemisorbed strongly on the Cu surface via the π-system of either of two CN groups.[27,28] The surface species formed by the chemisorption exhibits two split bands in the stretching region of nitrile groups because the two CN groups of SN are chemically inequivalent.[27] Second, the SN−Cu(I) coordination polymer is formed. Cu(I) has been reported to form a polymeric complex with dinitrile ligands.[27,29−31] For example, synthesis of bis(succinonitrile)copper(I) perchlorate was reported, and its crystal structure was fully determined via X-ray crystallography.[29] In contrast to the surface-bound SN, the SN moiety in the coordination polymer gives a single CN stretch peak.[27]

The Raman spectrum of the Cu electrode polarized in our SN-present electrolyte showed a single strong band of the C≡N stretching mode at 2293 cm^{-1} (Figure 3).[27] The weak bands

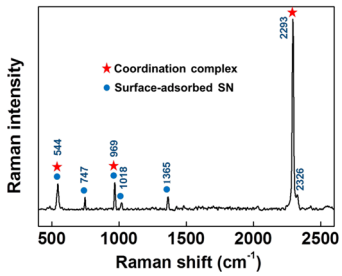

Figure 3. Raman spectrum of the copper electrode anodically polarized in the SN-present electrolyte used in Figure 2.

at 747, 1018, and 1365 cm^{-1} are assigned to C−C−C bending, CH_2 rocking, and CH_2 bending modes of the surface-adsorbed SN, respectively.[27] The amount of adsorbed SN, however, is expected to be negligible compared with that of the SN-based coordination polymer, when their weak intensities are considered. The other two weak bands at 544 and 969 cm^{-1} are attributed to the C−C−C bending and C−CN stretching modes, respectively, which result from either the coordination polymer or surface-adsorbed SN.[27] Therefore, we concluded that the SN moiety is definitely present on the anodically polarized Cu surface not as the surface-bound form but as the coordination polymer.

To quantify the formation of the coordination polymer, the mass change (ΔM) was measured during the sweeping potential of a Cu electrode (Figure 4). The mass accumulated per mole of electron transferred (mpe) is useful information for

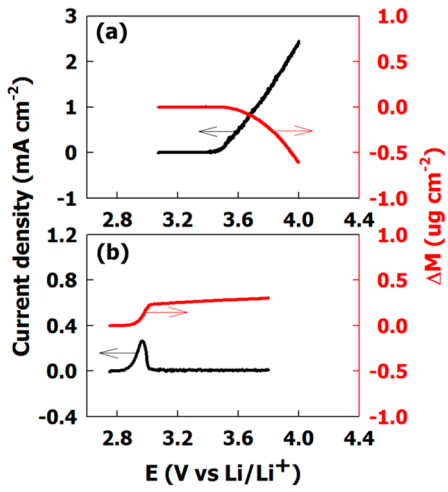

Figure 4. LSVs (black for the left ordinate) and concurrent mass change (red for the right ordinate) of copper electrodes with 1 M $LiPF_6$ in an EC/EMC mixture [1/2 (v/v)] containing no additive (a) or 3 wt % SN (b). The scan rate was 20 mV s^{-1}.

identifying the species deposited on the electrode during EQCM experiments:[32] mpe = $F(\Delta M/\Delta Q)$, where ΔQ is the change in charge involved in the electrochemical reaction causing the mass change and F is the Faraday constant. In the SN-absent electrolyte (Figure 4a), the mass of the Cu electrode is decreased along with an increase in the oxidation current during the anodic potential sweep. The mass change is caused by a loss of electrode mass by corrosion. The mpe of the Cu oxidation was determined to be −58. The value roughly corresponds to the molar weight of Cu (MW = 63.5), implying that Cu is oxidized mainly into Cu^+ rather than Cu^{2+} ions. The preferred oxidation to the monovalent species was also observed in a propylene carbonate solution.[22,23] On the other hand, a notable mass increase is observed near the peak potential in the SN-present electrolyte (Figure 4b). The mpe in the potential range was estimated to be +289. The mpe value is approximated by the increase in the molar weight of surface species from Cu to $Cu(SN)_2PF_6$: 305 = 368 [MW of $Cu(SN)_2PF_6$] − 63.5 [MW of Cu(I)]. Thus, the EQCM data, combined with the Raman result, clearly support the thought that the current peak in an SN-added electrolyte is associated with the formation of a $Cu(SN)_2PF_6$-type complex, which seems to be responsible for the suppression of further Cu corrosion.

On the basis of the obtained experimental results, the mechanism of Cu corrosion inhibition by SN is schematized in Figure 5. In the absence of SN, the Cu oxidation starts above 3.5 V (vs Li/Li^+). The main dissolution species are Cu^+ rather than Cu^{2+} ions as evidenced by the EQCM result (Figure 4a). In contrast, the Cu oxidation is initiated in the presence of SN as early as 2.8 V. The copper ions on the surface are combined by electronegative nitriles of SN, creating a coordination polymer composed of $Cu(SN)_2PF_6$. The surface SN−Cu complex layer suppresses further Cu dissolution, resulting in a peak current around 2.9 V. The surface layer eventually serves as a passive layer toward the Cu corrosion.

Overdischarge Protection by SN. On the basis of the formation of the Cu−SN complex on the Cu surface and its role as a corrosion inhibitor up to 4.5 V, we introduced SN as an electrolyte additive for commercial-grade LIBs (nominal

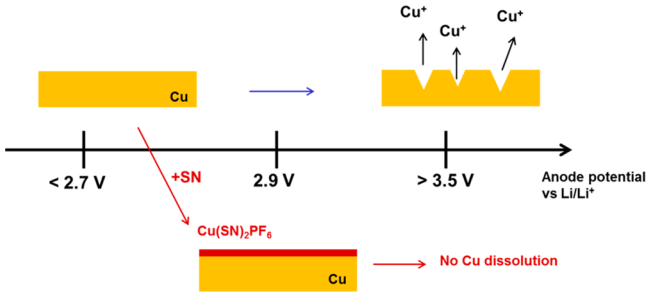

Figure 5. Schematic comparison of copper corrosion between SN-absent and SN-present electrolytes.

capacity of 750 mAh). The individual potentials of the cathode and anode were obtained in addition to the cell potential by means of three electrode measurements. The LIBs were overdischarged at three different discharge currents: 300 mA to 3 V, 3 mA to 2.7 V, and then 1 mA to 0 V. A smaller discharge current (1 mA) was applied at the final step to ensure the OD of the cells. The cell voltage profile of the SN-absent control cell exhibited a plateau around 0.25 V (Figure 6a). The

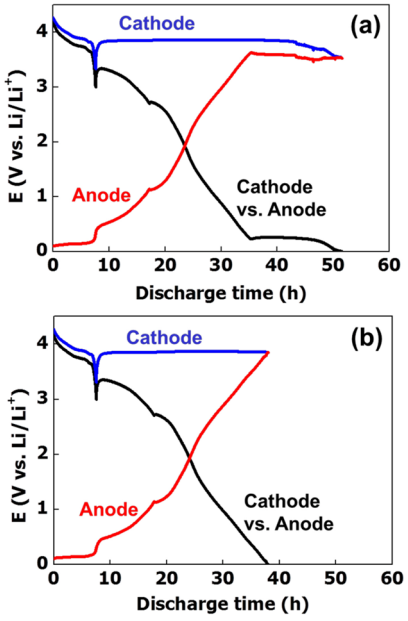

Figure 6. Potential profiles of 750 mAh $LiCoO_2$|graphite full cells with 1 M $LiPF_6$ in an EC/EMC mixture [1/2 (v/v)] containing no additive (a) or 3 wt % SN (b). Potentials were recorded for cathode vs reference (blue), anode vs reference (red), and cathode vs anode (black).

cell voltage change is primarily driven not by the cathode but by the anode, which is a typical OD behavior of cells in an anode-limiting configuration. The plateau region of the cell voltage corresponds to the point at which the anode voltage stays around 3.5 V due to anodic Cu dissolution. Cu corrosion continued until the cathode voltage decreased to meet the anode potential. In contrast, our SN-present cell exhibits no plateau region during the OD test (Figure 6b), its cell voltage decreasing monotonically to 0 V. Any indication of significant Cu oxidation was not observed as the anode voltage increased above 3.8 V to complete the OD procedure. The absence of Cu corrosion is ascribed to the passivation layer formed by SN on the Cu surface as confirmed above. The recovery ratio of discharge capacity after three repeated OD tests was estimated to be more than 98% in the SN-present cell (Figure 7 and

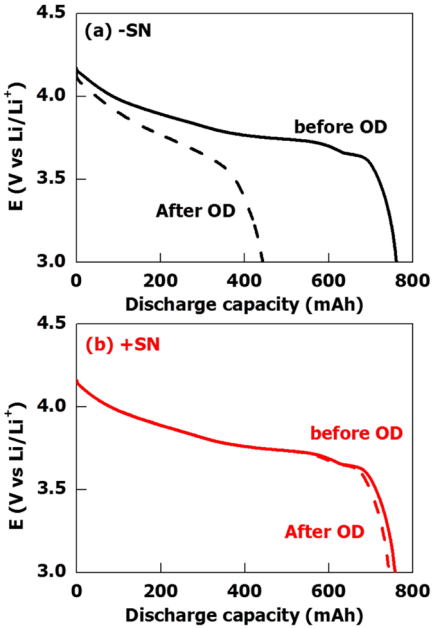

Figure 7. Potential profiles of the cells used in Figure 6 before and after three repeated OD tests. SN-absent (a) and SN-present (b) electrolytes were used. The discharge current was 0.2 C.

Figure S1 of the Supporting Information), guaranteeing the immunity toward the OD abuse. On the other hand, the recovery ratio of the SN-absent control cell is only 58% because of severe Cu dissolution.

Our strategy employing an electrolyte additive that induces an effective passivation on the Cu current collector is completely different from the previously reported OD protection methods based on cell balance control or redox shuttle additives.[12,13] It should be noted that the OD protection by SN is activated only when the anode voltage is forcibly increased to an abnormally high value (>2.9 V). Therefore, SN addition is hardly expected to alter anode performance under the normal operating condition. SN drove no significant change in discharge profiles between SN-absent and SN-present electrolytes before OD events (solid lines in panels a and b of Figure 7). In addition, our previous study has already shown that SN addition greatly enhances the thermal stability of $LiCoO_2$/graphite cells without any adverse effects in other cell performances.

Although SN has been revealed to be an excellent passivation agent of the Cu current collector for OD protection, there would be every possibility that SN is not the most ideal nitrile compound for Cu corrosion inhibition. It seems highly probable that the corrosion inhibition ability of nitrile-based compounds greatly depends on their molecular structure such as the number of nitrile groups (di- or mononitrile) and chain structure (length of the aliphatic chain or the presence of a double bond). Also, formation of the $Cu(SN)_2PF_6$-type complex and its solubility might be affected by the physicochemical properties of electrolytes. Some of these subjects are under investigation in our group, with the aim of exploring novel nitrile-based compounds that can surpass SN.

CONCLUSION

We investigated SN as a novel electrolyte additive for OD protection of LIBs. The presence of SN extended the oxidation stability of the copper current collector from 3.5 V (vs Li/Li^+) to >4.5 V. The corrosion inhibition by SN was attributed to formation of the surface passive layer composed of $Cu(SN)_2PF_6$ units. The enhanced corrosion resistance of the copper current collector allowed the OD protection of LIBs, which was confirmed through three-electrode measurements. In contrast to conventional LIBs suffering from huge capacity loss by the OD, the cells with SN were tuned to be totally immune to the OD abuse. The novel OD protection method described herein has critical advantages over the previous approaches. It requires no modification in the design and manufacturing process of LIBs, nor does it pose any limitation on the choice of cathode material. In addition, this study suggests corrosion inhibitors for metallic components of LIBs as a novel category of functional electrolyte additives, for the first time to the best of our knowledge, with the aim of expanding the reliability limit of the state-of-the-art LIBs.

ASSOCIATED CONTENT

Supporting Information

Potential profiles of three repeated overdischarges in the absence and presence of SN. This material is available free of charge via the Internet at http://pubs.acs.org.

AUTHOR INFORMATION

Corresponding Authors

*E-mail: philiphobi@hotmail.com.
*E-mail: dukelee@dgist.ac.kr.

Author Contributions

Y.-S.K. and S.-H.L. contributed equally to this work.

Notes

The authors declare no competing financial interest.

ACKNOWLEDGMENTS

This work was partly supported by MOTIE/KIAT through the Inter-ER Cooperation Projects (R0000491). H.L. is also grateful for the financial support from the IT R&D program of MOTIE/KEIT (10041856, Technology development for life improvement of high Ni composition cathode at high temperature) and by the DGIST MIREBraiN program.

REFERENCES

(1) Kim, T. H.; Park, J. S.; Chang, S. K.; Choi, S.; Ryu, J. H.; Song, H. K. *Adv. Energy Mater.* **2012**, *2*, 860−872.
(2) Xu, M.; Xing, L.; Li, W.; Zuo, X.; Shu, D.; Li, G. *J. Power Sources* **2008**, *184*, 427−431.
(3) Lee, H.; Lee, J. H.; Ahn, S.; Kim, H.-J.; Cho, J.-J. *Electrochem. Solid-State Lett.* **2006**, *9*, A307−A310.
(4) Xu, M.; Li, W.; Lucht, B. L. *J. Power Sources* **2009**, *193*, 804−809.
(5) Kim, Y. S.; Kim, T. H.; Lee, H.; Song, H. K. *Energy Environ. Sci.* **2011**, *4*, 4038−4045.
(6) Zhang, H.; Xia, Q.; Wang, B.; Yang, L.; Wu, Y.; Sun, D.; Gan, C.; Luo, H.; Bebeda, A.; Ree, T. v. *Electrochem. Commun.* **2009**, *11*, 526−529.
(7) Arora, P.; White, R. E.; Doyle, M. *J. Electrochem. Soc.* **1998**, *145*, 3647−3667.
(8) Li, H. F.; Gao, J. K.; Zhang, S. L. *Chin. J. Chem.* **2008**, *26*, 1585−1588.
(9) Maleki, H.; Howard, J. N. *J. Power Sources* **2006**, *160*, 1395−1402.
(10) Wu, M.-S.; Lin, C.-Y.; Wang, Y.-Y.; Wan, C.-C.; Yang, C. R. *Electrochim. Acta* **2006**, *52*, 1349−1357.
(11) Zhao, M. C.; Kariuki, S.; Dewald, H. D.; Lemke, F. R.; Staniewicz, R. J.; Plichta, E. J.; Marsh, R. A. *J. Electrochem. Soc.* **2000**, *147*, 2874−2879.
(12) Chen, J.; Buhrmester, C.; Dahn, J. R. *Electrochem. Solid-State Lett.* **2005**, *8*, A59−A62.
(13) Lee, H.; Chang, S. K.; Goh, E. Y.; Jeong, J. Y.; Lee, J. H.; Kim, H. J.; Cho, J. J.; Hong, S. T. *Chem. Mater.* **2008**, *20*, 5−7.
(14) Aurbach, D.; Eineli, Y.; Markovsky, B.; Zaban, A.; Luski, S.; Carmeli, Y.; Yamin, H. *J. Electrochem. Soc.* **1995**, *142*, 2882−2890.
(15) Tang, M.; Miyazaki, K.; Abe, T.; Newman, J. *J. Electrochem. Soc.* **2012**, *159*, A634−A641.
(16) Tang, M.; Newman, J. *J. Electrochem. Soc.* **2012**, *159*, A1922−A1927.
(17) Antonijevic, M. M.; Petrovic, M. B. *Int. J. Electrochem. Sci.* **2008**, *3*, 1−28.
(18) dos Santos, L. M. M.; Lacroix, J. C.; Chane-Ching, K. I.; Adenier, A.; Abrantes, L. M.; Lacaze, P. C. *J. Electroanal. Chem.* **2006**, *587*, 67−78.
(19) Finsgar, M.; Milosev, I. *Corros. Sci.* **2010**, *52*, 2737−2749.
(20) Fonsati, M.; Zucchi, F.; Trabanelli, C. *Electrochim. Acta* **1998**, *44*, 311−322.
(21) Herrasti, P.; del Rio, A. L.; Recio, J. *Electrochim. Acta* **2007**, *52*, 6496−6501.
(22) Kawakita, J.; Kobayashib, K. *J. Power Sources* **2001**, *101*, 47−52.
(23) Klunker, J.; Schafer, W. *J. Electroanal. Chem.* **1999**, *466*, 107−116.
(24) Myung, S. T.; Hitoshi, Y.; Sun, Y. K. *J. Mater. Chem.* **2011**, *21*, 9891−9911.
(25) Myung, S. T.; Sasaki, Y.; Sakurada, S.; Sun, Y. K.; Yashiro, H. *Electrochim. Acta* **2009**, *55*, 288−297.
(26) Zhao, M. C.; Dewald, H. D.; Lemke, F. R.; Staniewicz, R. J. *J. Electrochem. Soc.* **2000**, *147*, 3983−3988.
(27) Loo, B. H.; Lee, Y. G.; Frazier, D. O. *J. Phys. Chem.* **1985**, *89*, 4672−4676.
(28) Steiner, U. B.; Caseri, W. R.; Suter, U. W. *Langmuir* **1992**, *8*, 2771−2777.
(29) Blount, J.; Freeman, H.; Hemmerich, P.; Sigwart, C. *Acta Crystallogr.* **1969**, *B25*, 1518−1524.
(30) Heller, M.; Sheldrick, W. S. *Z. Anorg. Allg. Chem.* **2004**, *630*, 1869−1874.
(31) Inada, Y.; Niwa, Y.; Iwata, K.; Funahashi, S.; Ohtaki, H.; Nomura, M. *J. Mol. Liq.* **2006**, *129*, 18−24.
(32) Aurbach, D.; Zaban, A.; Ein-Eli, Y.; Weissman, I.; Chusid, O.; Markovsky, B.; Levi, M.; Levi, E.; Schechter, A.; Granot, E. *J. Power Sources* **1997**, *68*, 91−98.